

Triptolide reduces ischemia/reperfusion injury in rats and H9C2 cells via inhibition of NF- κ B, ROS and the ERK1/2 pathway

BIN YANG^{1,2}, PING YAN³, GUANG-ZHAO YANG⁴, HUI-LI CAO², FEI WANG² and BAO LI^{1,2}

¹Department of Cardiovascular Medicine, The Second Affiliated Hospital of Shanxi Medical University, Taiyuan, Shanxi 030001; ²Department of Cardiovascular Medicine, Shanxi Cardiovascular Hospital, Taiyuan, Shanxi 030024;

³Department of Biochemistry and Molecular Biology, Shanxi Medical University, Taiyuan, Shanxi 030001;

⁴Department of Cardiovascular Medicine, The First Affiliated Hospital of Shanxi Medical University, Taiyuan, Shanxi 030012, P.R. China

Received June 22, 2016; Accepted January 12, 2018

DOI: 10.3892/ijmm.2018.3537

Abstract. Myocardial ischemia/reperfusion (I/R) induces cardiac cell injury; however, the mechanism underlying cardiac damage remains unclear. A previous study demonstrated that triptolide (TP) exerts protective effects against I/R in cerebral cells. The present study aimed to evaluate the protective effects of TP on cardiac cells, and investigated the potential mechanisms involved in I/R-induced damage. Rats and cardiac H9C2 cells undergoing I/R were pretreated with TP, and cell damage was assessed *in vivo* and *in vitro*. Hematoxylin and eosin and terminal deoxynucleotidyl-transferase-mediated dUTP nick end labeling staining were employed to evaluate I/R injury in rat cardiac tissue. Inflammatory factors, including tumor necrosis factor- α , interleukin (IL)-1 β and IL-6, were detected by ELISA. Biochemical analyses were performed to evaluate the bioactivity of superoxide dismutase, malondialdehyde and catalase. In addition, viability of H9C2 cells was measured using the Cell Counting kit 8 assay. Flow cytometry was used to evaluate cell apoptosis and reactive oxygen species (ROS) generation. Furthermore, the expression levels of proteins associated with apoptosis, peroxide and inflammation were measured using western blot analysis. H9C2 cells were also treated with *N*-acetylcysteine and pyrrolidine dithiocarbamate, and cell injury was assessed after peroxidation or I/R. The results demonstrated that TP exerted a significant protective effect on cardiac cells *in vivo* and *in vitro*. TP reduced the inflammatory response, as determined by nuclear factor- κ B inhibition. In

addition, TP decreased ROS-mediated lipid peroxidation, and reduced ROS generation. TP also inhibited cell apoptosis by activating the extracellular signal-regulated kinase 1/2 pathway. In conclusion, TP may protect cardiac cells from I/R injury; the potential protective mechanisms of TP against I/R include anti-inflammatory action, antioxidation and apoptotic resistance.

Introduction

Myocardial ischemia refers to reduced cardiac perfusion, which leads to abnormal oxygen reduction and energy metabolism, thus resulting in cardiac pathology (1). Under normal conditions, the myocardial oxygen uptake rate is as high as ~70%, in order to guarantee normal myocardial function, whereas myocardial ischemia occurs when the balance between myocardial blood supply and demand is broken, which is caused by numerous factors, including coronary heart disease (2). The prevalence of myocardial ischemia has been reported to be increasing worldwide, and it is a common and frequently encountered disease in middle-aged and elderly individuals (2). Thrombolysis, interventional therapy and coronary artery bypass grafting may be regularly applied for the management of serious myocardial ischemia (3,4). In addition, blood flow reperfusion leads to temporary survival of cardiac cells in the ischemic region and recovery of damaged tissue; however, the narrow therapeutic time window for these therapies may result in the occurrence of ischemia/reperfusion (I/R) injury. I/R injury may induce the disordered synthesis of mitochondrial energy and Ca²⁺ homeostasis, and the release of free radicals and inflammatory cytokines, eventually leading to myocardial cell apoptosis and organ damage (5-7). Due to its ability to induce irreversible damage to cardiac cells, I/R injury is considered a critical issue in the treatment of ischemic stroke.

In a previous study, anti-inflammatory agents were reported to reduce tissue damage and protect cells from ischemia (8). Triptolide (TP) is extracted from the traditional Chinese medicinal plant *Tripterygium wilfordii* Hook F, and is a bioactive ingredient with anti-inflammatory activity, which may be used to treat numerous disorders, including arthritis, pulmonary hypertension and traumatic brain injury (9-12). The inhibitory effects of TP on the production of inflammatory cytokines

Correspondence to: Dr Bao Li, Department of Cardiovascular Medicine, The Second Affiliated Hospital of Shanxi Medical University, 382 Wuyi Road, Taiyuan, Shanxi 030001, P.R. China
E-mail: libaoxys@163.com

Dr Ping Yan, Department of Biochemistry and Molecular Biology, Shanxi Medical University, Taiyuan, 56 Xinjian Road, Shanxi 030001, P.R. China
E-mail: yangbxys@163.com

Key words: ischemia/reperfusion injury, triptolide, inflammatory response, lipid peroxidation, cell apoptosis

in various cell lines has been determined in *in vitro* studies, thus suggesting the potential use of TP in the treatment of I/R injury (13-16). The protective effects of TP on cardiac cells against I/R injury have rarely been reported. Therefore, in the present study, a rat myocardial I/R model was used to evaluate the protective effects of TP on I/R. Furthermore, the H9C2 cardiac cell line was used to explore the potential mechanism underlying the protective effects of TP on I/R injury.

Materials and methods

Animal I/R model. Langendorff non-circulatory perfusion was employed to evaluate the protective effects of TP against I/R in rat cardiac tissues. Krebs-Henseleit (KH) buffer was equilibrated with 95% O₂ and 5% CO₂ at pH 7.4, and was flushed continually at 37°C. A total of 36 rats were randomly grouped into six and were anesthetized via intraperitoneal injection of heparin sodium (1,000 U/kg) and 10% chloral hydrate (350 mg/kg) for 20 min. The hearts were rapidly excised and placed in ice-cold KH buffer. The aorta of the control group was fixed with an infusion tube and perfused at a constant perfusion pressure of 75 mmHg using a Langendorff non-circulatory perfusion pump, for 170 min. The other groups underwent ischemia for 30 min following perfusion for 80 min, and were then reperfused for 60 min. A fluid-filled balloon was inserted into the left ventricle and attached to a pressure transducer. A cardiac pacemaker was used to generate a heart rate of 280 beats/min. The present study was approved by the Institutional Animal Care and Use Committee (IACUC-20130315-01).

Histology and terminal deoxynucleotidyl-transferase-mediated dUTP nick end labeling (TUNEL) staining. Cardiac tissues were fixed in 10% formalin for 48 h. Tissues were dehydrated using ethanol and were cleared with xylene, after which they were embedded in paraffin and cut into 4-7 μm sections. Slides of the tissue sections were then deparaffinized, dehydrated and stained with hematoxylin and eosin (H&E). Infiltrating neutrophils were identified and visualized under a microscope.

For TUNEL staining, the slides were deparaffinized and dehydrated as aforementioned. The sections were digested for 40 min, and were then incubated with 50 μl TUNEL buffer at 37°C for 1 h, and 50 μl POD at 37°C for 30 min, respectively. Finally, the slides were stained with DAB for 3-10 min, sections were visualized under a microscope and apoptotic rate was calculated.

Cell culture. H9C2 cells were cultured in Dulbecco's modified Eagle's medium (DMEM) supplemented with 10% fetal calf serum and 1% x100 mycillin at 37°C in an atmosphere containing 5% CO₂. To study the effects of TP on I/R cells, H9C2 cells were then digested, seeded into 96-well plates (3x10³ cells/well) and divided into five groups in triplicate. The control group was incubated in normal culture medium. The I/R group was transferred into sugar- and serum-free DMEM, and was incubated at 37°C in an atmosphere containing 5% CO₂ and 1% O₂ for 2 h, after which, cells were transferred into normal DMEM and were cultured for 6 h. The TP groups were treated with various concentrations of TP for 1 h, and underwent hypoxia-reoxygenation as described in the I/R group. Furthermore, cultured cells were treated with *N*-acetylcysteine (NAC) or pyrrolidine

dithiocarbamate (PDTTC), in order to investigate the mechanisms underlying the protective effects of TP against I/R injury. To study the effects of TP on H₂O₂-treated cells, cells were pretreated with NAC, PDTTC or TP for 1 h, and then treated with 100 μM H₂O₂ for 24 h. Cultured and treated cells were prepared for further experiments.

ELISA. The ELISA method was used to measure the expression levels of tumor necrosis factor (TNF)-α, interleukin (IL)-1β and IL-6 in cardiac tissues and H9C2 cells by determining the absorbance at 450 nm. Briefly, ~10 mg cardiac tissues or 100 μl cultured cells were processed according to the manufacturers' protocols. TNF-α, IL-1β and IL-6 concentrations were calculated according to the standard curve, which was generated from a series of known concentrations of standard bovine serum albumin.

Biochemical analysis. Cardiac antioxidant status was determined by measuring cardiac superoxide dismutase (SOD) content. Tissue samples were homogenized in 100 mmol/l Tris-HCl buffer and were centrifuged at 10,000 x g for 20 min. SOD, malondialdehyde (MDA) and catalase (CAT) levels were assessed using commercial kits (Nanjing Jiancheng Bioengineering Institute, Nanjing, China). Total protein concentration in heart homogenates was determined using the Coomassie blue method.

Cell Counting kit (CCK)-8 assay. Cultured and treated H9C2 cells were treated with 100 μl serum-free DMEM containing 10% CCK-8 (Dojindo Molecular Technologies, Inc., Kumamoto, Japan) at 37°C for 1 h in an atmosphere containing 5% CO₂. The optical density of cell suspensions was measured at 450nm using a spectrophotometer, in order to evaluate the viability of H9C2 cells.

Cell apoptosis assay. Cultured and treated H9C2 cells were treated with 0.25% trypsin, in order to form a single cell suspension, and were washed with 10% PBS and centrifuged at 1,000 x g for 5 min. The supernatant was discarded and cells were then incubated with the Annexin V-fluorescein isothiocyanate (FITC) apoptosis detection kit (BD Biosciences, San Diego, CA, USA) for 10 min at room temperature in the dark. Cell apoptotic rate was measured and data were obtained using flow cytometry (FACSCalibur; BD Biosciences).

DNA fragmentation assay. Cultured cells were fixed with 3% paraformaldehyde and incubated at room temperature for 5 min. Subsequently, the cells were air-dried and stained with 10 ml Hoechst 33258 (Beyotime Institute of Biotechnology, Jiangsu, China) for 10 min, followed by the addition of 50% glycerol containing 20 mmol/l citric acid and 50 mmol/l orthophosphate. A fluorescence microscope was used to evaluate nuclear morphology.

Reactive oxygen species (ROS) assay. Cultured cells were washed with PBS and digested using trypsin following treatment with PA for 24 h; followed by centrifugation at 1,500 rpm for 10 min. Cells were then collected and resuspended in staining buffer containing 50 μM dihydroethidium (Wegelasi Biotechnology Co., Ltd.). ROS was measured by flow cytometry.

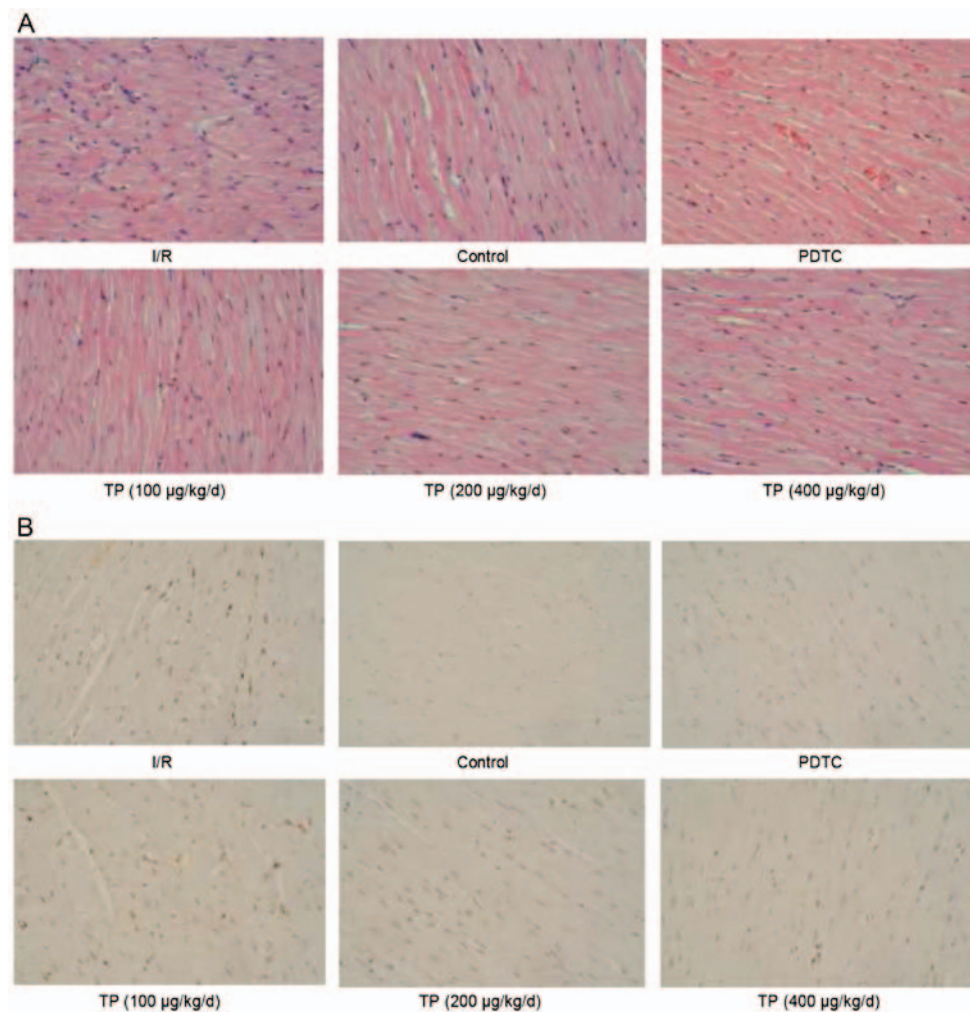


Figure 1. Immunohistochemical analysis of hearts subjected to sham surgery for 30 min of ischemia and 60 min of reperfusion. (A) Effects of TP on cardiac tissue injury after I/R were evaluated by hematoxylin and eosin staining. (B) Terminal deoxynucleotidyl-transferase-mediated dUTP nick end labeling staining was used to evaluate the effects of TP on cell apoptosis after I/R. I/R, ischemia/reperfusion; PDTC, pyrrolidine dithiocarbamate; TP, triptolide.

Western blot analysis. Briefly, 20 mg tissue samples were cut into pieces and proteins were extracted using 250 μ l radioimmunoprecipitation assay buffer (Shanghai Solarbio Science & Technology Co., Ltd., Shanghai, China) containing 0.01% protease inhibitor cocktail (Sigma-Aldrich; Merck KGaA, Darmstadt, Germany). In addition, cultured cells were washed twice with 1X PBS, and were lysed at 4°C. Furthermore, nuclear and plasma proteins were extracted from tissue samples using the NE-PER kit (Thermo Fisher Scientific, Inc., Waltham, MA, USA). Subsequently, samples were centrifuged at 12,000 \times g for 15 min at 4°C and the supernatants were collected. The bicinchoninic acid protein quantification kit (Thermo Fisher Scientific, Inc.) was used to quantify protein contents. Tissue and cell proteins were separated by 15% (80 μ g/well) or 10% (25 μ g/well) SDS-PAGE, respectively, and proteins were electrophoretically transferred to a nitrocellulose filter membrane (EMD Millipore, Billerica, MA, USA). Blots were blocked with 5% skim milk at room temperature for 1 h, and were then incubated with anti-B-cell lymphoma 2 (Bcl2) and Bcl2-associated X protein (Bax) (Santa Cruz Biotechnology, Inc., Santa Cruz, CA), caspase-3, lectin-like oxidized low-density lipoprotein receptor-1 (LOX-1) and inducible nitric oxide synthase (iNOS) (Abcam, Cambridge, UK), cyclooxygenase (COX)2, nuclear factor (NF)- κ B, phosphory-

lated (p)-NF- κ B, NF- κ B inhibitor α (I κ B α), p-I κ B α , extracellular signal-regulated kinase (ERK)1/2, p-ERK1/2 and GAPDH antibodies (Cell Signaling Technology, Inc., Danvers, MA, USA). and were incubated with goat anti-mouse or anti-rabbit secondary antibodies (Beyotime Institute of Biotechnology). Enhanced chemiluminescence (Thermo Fisher Scientific, Inc.) was used to visualize the blots.

Statistical analysis. Data are presented as the means \pm standard deviation of at least three independent replicates. The results were analyzed using analysis of variance followed by the Tukey multiple comparisons test. GraphPad Prism 5.0 software (GraphPad Software, Inc., La Jolla, CA, USA) was used to perform data analysis. $P < 0.05$ was considered to indicate a statistically significant difference.

Results

TP inhibits rat myocardial cell apoptosis. H&E and TUNEL staining were performed to evaluate the effects of I/R on control and TP-treated cardiac tissues. As shown in Fig. 1A, cells in the I/R group exhibited swelling, necrosis and degeneration, alongside marked neutrophil infiltration. Conversely, less severe

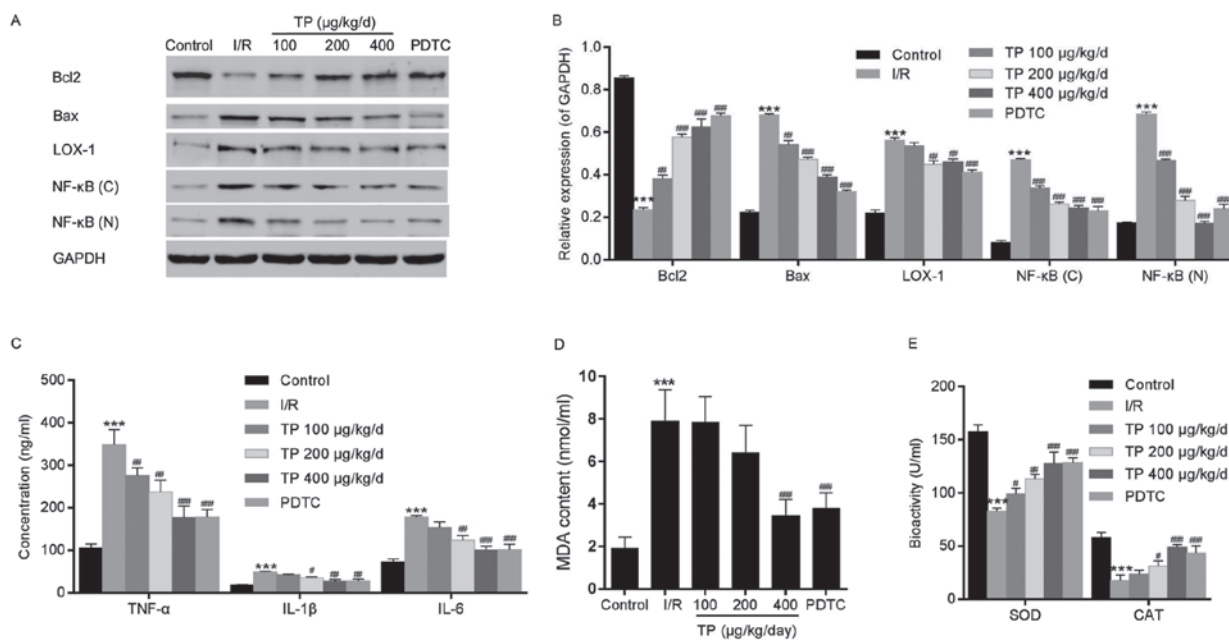


Figure 2. Western blot analysis and ELISA were performed to investigate the mechanisms underlying the protective effects of TP against I/R in cardiac tissues. (A and B) Western blot analysis was used to measure the protein expression levels of Bcl2, Bax, LOX-1 and NF-κB. (C) ELISA analysis was used to determine the inhibitory effects of TP on the expression of inflammation-associated proteins, TNF- α , IL-1 β and IL-6. (D and E) Biochemical analyses revealed the alterations in SOD, MDA and CAT. *** P <0.001, compared with the control group. # P <0.05, ## P <0.01, ### P <0.001, compared with the I/R group (n =6). Bax, Bcl2-associated X protein; Bcl2, B-cell lymphoma 2; (C), cytoplasmic; CAT, catalase; IL, interleukin; I/R, ischemia/reperfusion; LOX-1, lectin-like oxidized low-density lipoprotein receptor-1; MDA, malondialdehyde; (N), nuclear; NF-κB, nuclear factor-κB; PDTC, pyrrolidine dithiocarbamate; SOD, superoxide dismutase; TNF- α , tumor necrosis factor- α ; TP, triptolide.

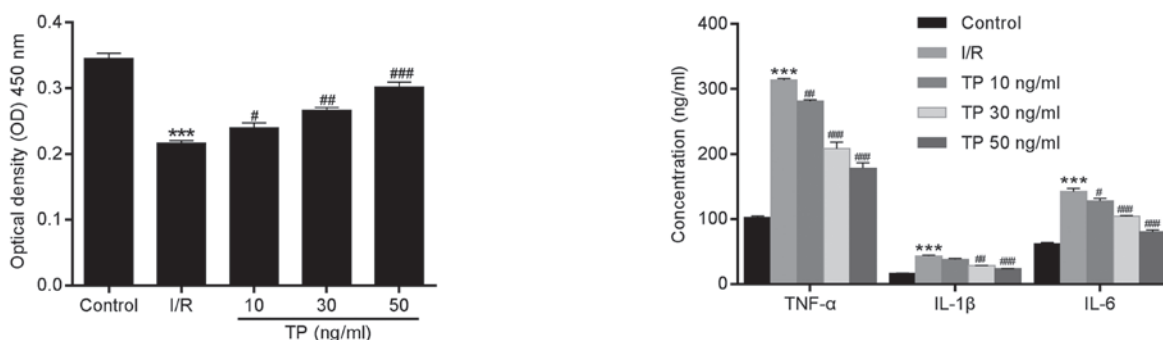


Figure 3. Viability of H9C2 cells was determined using the Cell Counting kit-8 assay 12 h after 2 h of ischemia and 6 h of reperfusion. Cell viability of H9C2 cells was improved by TP in a dose-dependent manner. *** P <0.001, compared with the control group. # P <0.05, ## P <0.01 and ### P <0.001 compared with the I/R group (n =3). TP, triptolide; I/R, ischemia/reperfusion.

Figure 4. Expression of inflammatory factors in H9C2 cells was determined using ELISA after 2 h of ischemia and 6 h of reperfusion. TP inhibited the expression of inflammatory factors, TNF- α , IL-1 β and IL-6, in a dose-dependent manner. *** P <0.001, compared with the control group. # P <0.05, ## P <0.01 and ### P <0.001, compared with the I/R group (n =3). IL, interleukin; I/R, ischemia/reperfusion; TNF- α , tumor necrosis factor- α ; TP, triptolide.

cell necrosis was determined, and stained cells exhibited normal architecture in the PDTC- and TP-treated groups, thus indicating that I/R induced cell damage, whereas TP exerted protective effects against I/R. TUNEL staining demonstrated that I/R induced cell apoptosis (Fig. 1B); apoptotic cells were stained brown in the I/R group. The number of positively stained cells was reduced in the TP-treated groups, thus indicating the inhibitory effects of TP against I/R-induced cell apoptosis. In addition, Bcl2 was increased and Bax was decreased, as determined by western blot analysis, indicating that cell apoptosis was inhibited by TP compared with in the I/R group (Fig. 2A and B).

TP inhibits the inflammatory response in rat myocardial cells. TNF- α , IL-1 β and IL-6 were evaluated using ELISA,

in order to investigate the inflammatory response following I/R in rat myocardial cells. Significant increases in the expression levels of TNF- α , IL-1 β and IL-6 were detected in the I/R group, whereas these increased levels were attenuated in the TP-treated groups in a dose-dependent manner (Fig. 2C). Similarly, the relative nuclear and plasma protein expression levels of NF-κB were decreased in the TP-treated groups compared with in the I/R group (Fig. 2A and B).

TP protects rat myocardial cells from peroxidation. The levels of cardiac enzymes, SOD, MDA and CAT, were measured to evaluate the oxidative damage caused by I/R (Fig. 2D and E). Although higher levels of SOD and MDA were detected in the I/R and TP-treated groups compared

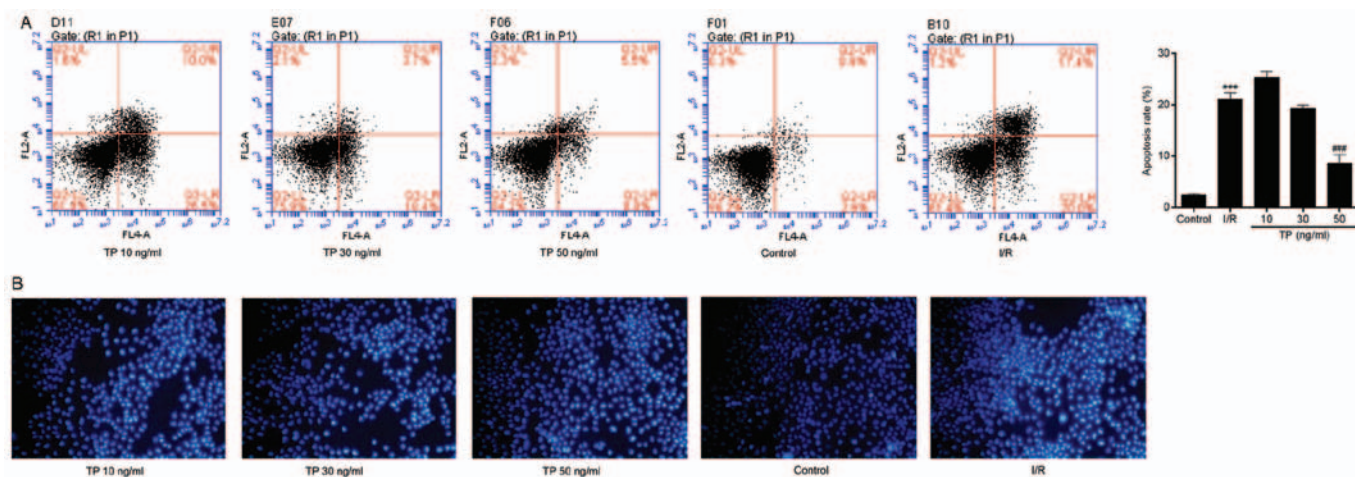


Figure 5. Cell apoptosis was measured by flow cytometry after 2 h of ischemia and 6 h of reperfusion. (A) Early apoptotic cells were detected using Annexin V/propidium iodide double staining, and are presented in the lower right quadrant. **** $P < 0.001$, compared with the control group. *** $P < 0.001$, compared with the I/R group (n=3). (B) Apoptosis of H9C2 cells was observed using Hoechst 33258 fluorescence staining. Morphology of apoptotic cells exhibited chromosomal condensation and nuclear fragmentation. I/R, ischemia/reperfusion; TP, triptolide.

with in the control group, the enzymatic activities of SOD and MDA were reduced in the TP-treated groups compared with in the I/R group in a dose-dependent manner. In addition, CAT activity exhibited almost no alteration between the I/R and TP-treated groups. Furthermore, LOX-1 was measured by western blot analysis; the protein expression levels of LOX-1 were attenuated compared with in the I/R group (Fig. 2A and B), thus suggesting that TP exerts protective effects against I/R-induced peroxidation.

TP improves the viability of H9C2 cells. In order to investigate the possible mechanisms underlying the protective effects of TP against I/R injury in cardiac cells, an *in vitro* study was performed using H9C2 cells. The CCK-8 assay was performed to evaluate the viability of H9C2 cells after 2 h of ischemia and 6 h of reperfusion. Compared with in the I/R group, cell proliferation in the TP-treated groups was increased in a dose-dependent manner (Fig. 3), thus indicating the improved viability of H9C2 cells following TP treatment.

TP reduces inflammation in H9C2 cells. ELISA was used to measure the expression levels of TNF- α , IL-1 β and IL-6 in H9C2 cells after I/R. Similar to the expression levels of TNF- α , IL-1 β and IL-6 detected in cardiac tissues, the expression levels of these proteins were significantly increased in the I/R group compared with in the control group, and were decreased in the TP-treated groups compared with in the I/R group in a dose-dependent manner (Fig. 4).

TP inhibits apoptosis of H9C2 cells. Flow cytometry was used to evaluate apoptosis in the control and TP-treated H9C2 cells. I/R-induced cell apoptosis was detected using Annexin V-FITC/propidium iodide (PI) double staining (Fig. 5A). The apoptotic rate was calculated from the percentage of early apoptotic cells presented in the lower right quadrant of the histograms. The apoptotic rate was dose-dependently reduced in the TP-treated H9C2 cells compared with in the I/R group, thus revealing the inhibitory effect of TP against I/R. Hoechst 33258 staining was also used

to morphologically detect apoptosis of H9C2 cells through fluorescence staining (Fig. 5B). Nuclear fragmentation and chromosomal condensation were improved in the cells treated with various concentrations of TP compared with in the I/R group. Furthermore, apoptosis of H9C2 cells was measured, in order to evaluate the protective effects of TP against H₂O₂-induced peroxidation. As shown in Fig. 6A and B, the apoptotic rate was increased in the H₂O₂ and I/R groups, whereas the apoptotic rate was significantly reduced in the NAC-, PDTC- and TP-treated groups.

TP reduces ROS generation. ROS are produced by the mitochondrial electron transport chain in cells, and are involved in cell apoptosis via the regulation of caspases. ROS generation may be detected using dihydroethidium, which has free access into live cells through the cell membrane. As shown in Fig. 7A, compared with in the control group, the fluorescence intensity of ROS was increased in H9C2 cells in the I/R group. However, there was a significant dose-dependent decrease in ROS generation in the TP-treated groups compared with in the I/R group. In addition, reductions in SOD, CAT and MDA expression in the TP-treated groups indicated the antioxidative effects of TP (Fig. 7B and C). As presented in Fig. 8, TP exerted protective effects against H₂O₂-induced peroxidation, according to the decreased fluorescence intensity of ROS in NAC-, PDTC- and TP-treated groups.

Effects of TP on protein expression in H9C2 cells. The expression levels of inflammatory-associated proteins, NF- κ B and I κ B α , were measured by western blot analysis (Fig. 9A and B), as was the expression of iNOS (Fig. 9A and C). I κ B α was downregulated in the I/R group, whereas NF- κ B was upregulated. Conversely, the expression levels of NF- κ B were decreased and I κ B α was increased in the TP-treated groups in a dose-dependent manner; similar findings were detected in the NAC and PDTC groups. The phosphorylation of I κ B α and NF- κ B was increased in the I/R group, but decreased in the TP-treated groups (Fig. 10). In addition, upregulation of iNOS was detected following I/R, whereas in the TP-treated

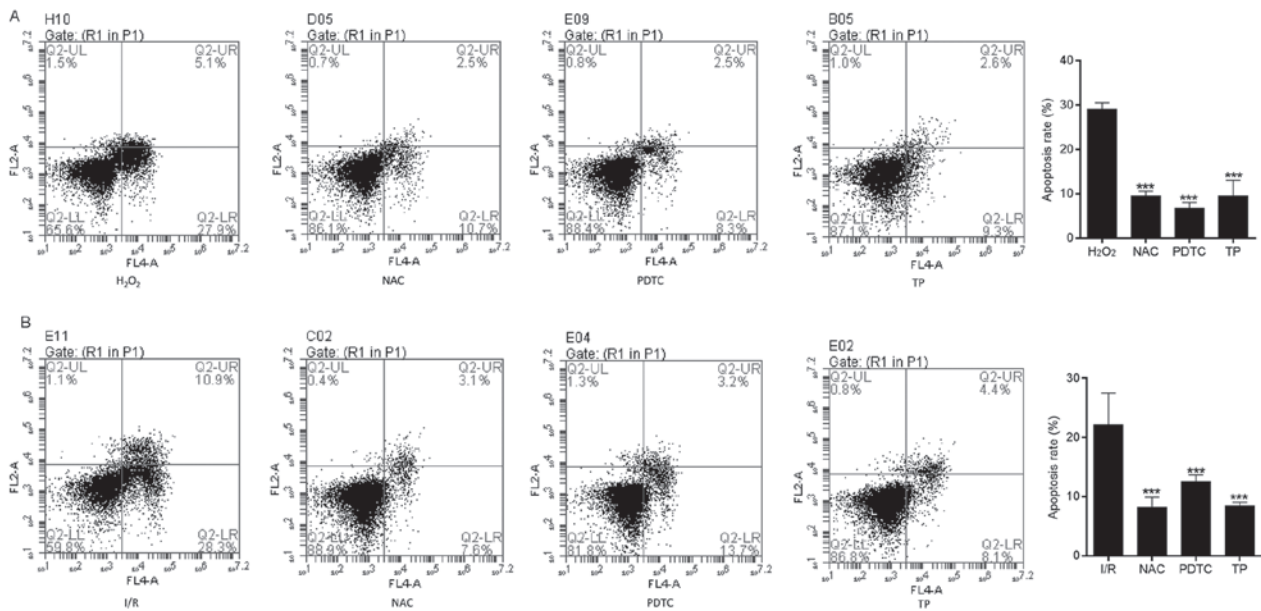


Figure 6. Cell apoptosis was measured by flow cytometry, in order to evaluate the protective effects of TP against H₂O₂. (A) Early apoptotic cells were determined following treatment with H₂O₂ for 24 h using Annexin V/PI double staining, and are presented in the lower right quadrant. ***P<0.001, compared with the H₂O₂ group (n=3). (B) Early apoptotic cells were determined using Annexin V/PI double staining after 2 h of ischemia and 6 h of reperfusion. ***P<0.001, compared with the I/R group. H₂O₂, hydrogen peroxide; I/R, ischemia/reperfusion; NAC, N-acetylcysteine; PDTC, pyrrolidine dithiocarbamate; PI, propidium iodide; TP, triptolide.

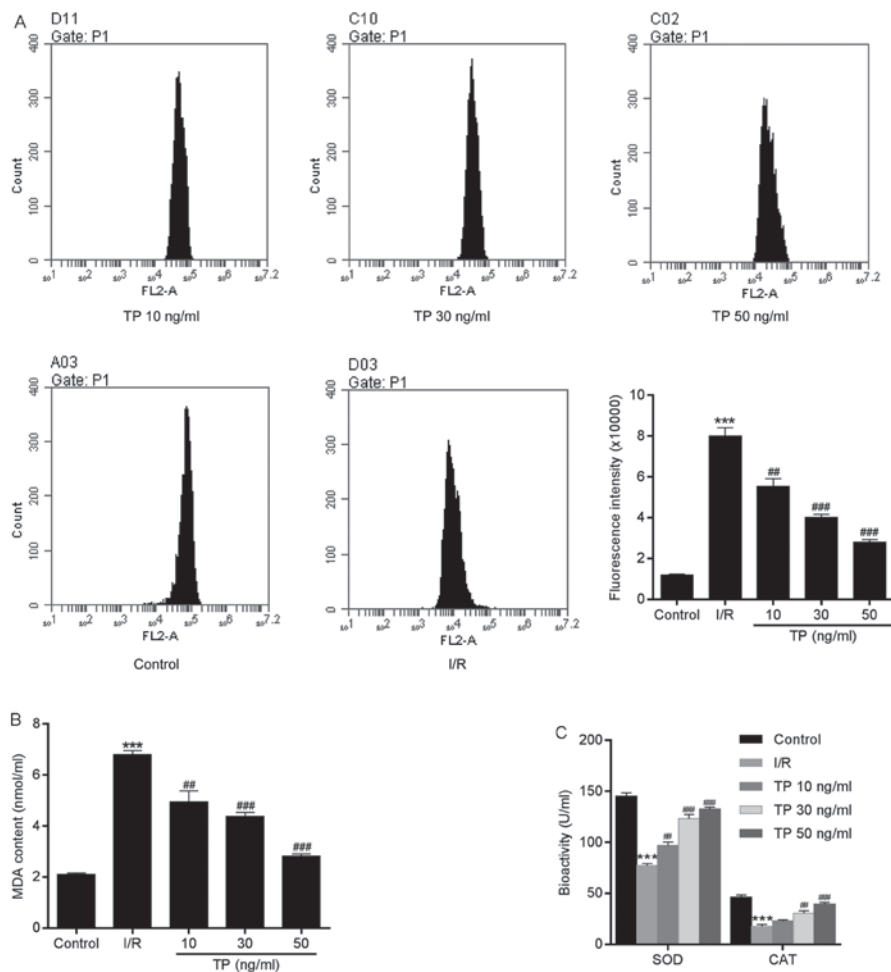


Figure 7. Generation of ROS in H9C2 cells during the process of cell apoptosis. (A) Compared with in the control group, ROS, as measured using dihydroethidium, was significantly decreased in TP-treated cells in a dose-dependent manner. (B and C) TP exerted protective effects against I/R via SOD, MDA and CAT. ***P<0.001, compared with the control group. ##P<0.01, ###P<0.001, compared with the I/R group (n=3). CAT, catalase; I/R, ischemia/reperfusion; MDA, malondialdehyde; ROS, reactive oxygen species; SOD, superoxide dismutase; TP, triptolide.

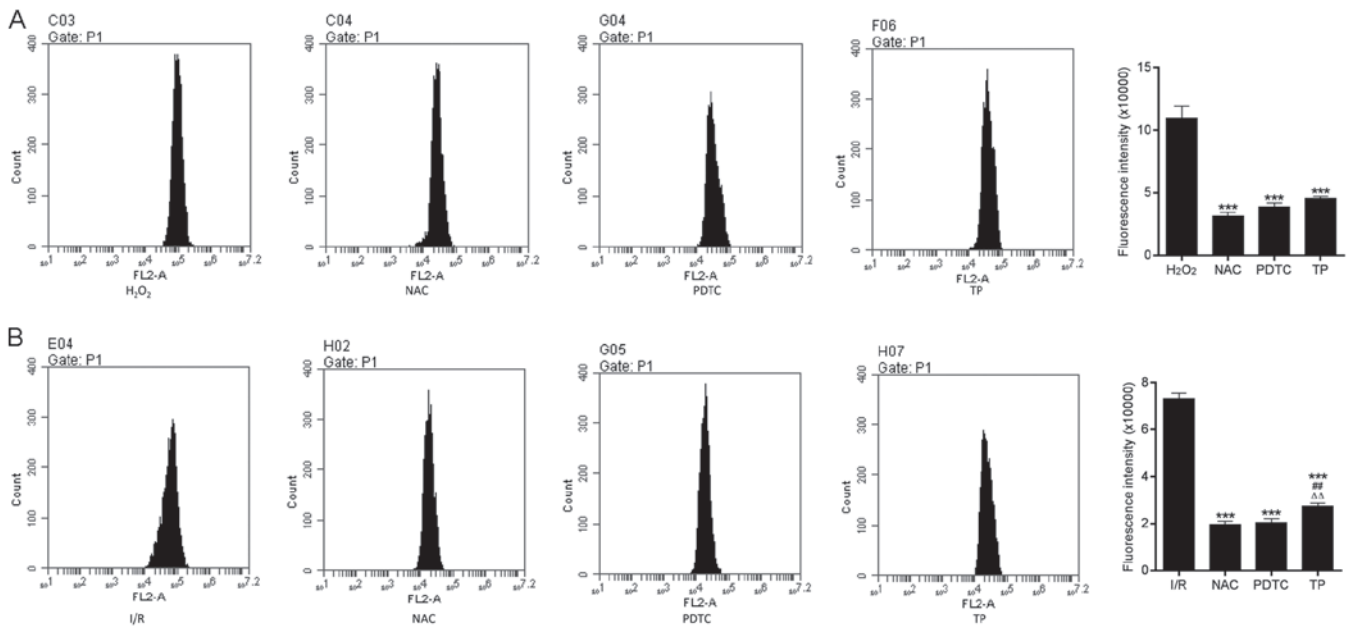


Figure 8. ROS generation in H9C2 cells during the process of cell apoptosis. (A) ROS generation was measured in H9C2 cells treated with H₂O₂ for 24 h. ***P<0.001, compared with the H₂O₂ group. (B) ROS generation in H9C2 cells after 2 h of ischemia and 6 h of reperfusion. ***P<0.001, compared with the I/R group. #P<0.01, compared with the NAC group. $\Delta\Delta$ P<0.01, compared with the PDTC group (n=3). H₂O₂, hydrogen peroxide; I/R, ischemia/reperfusion; NAC, N-acetylcysteine; PDTC, pyrrolidine dithiocarbamate ROS, reactive oxygen species; TP, triptolide.

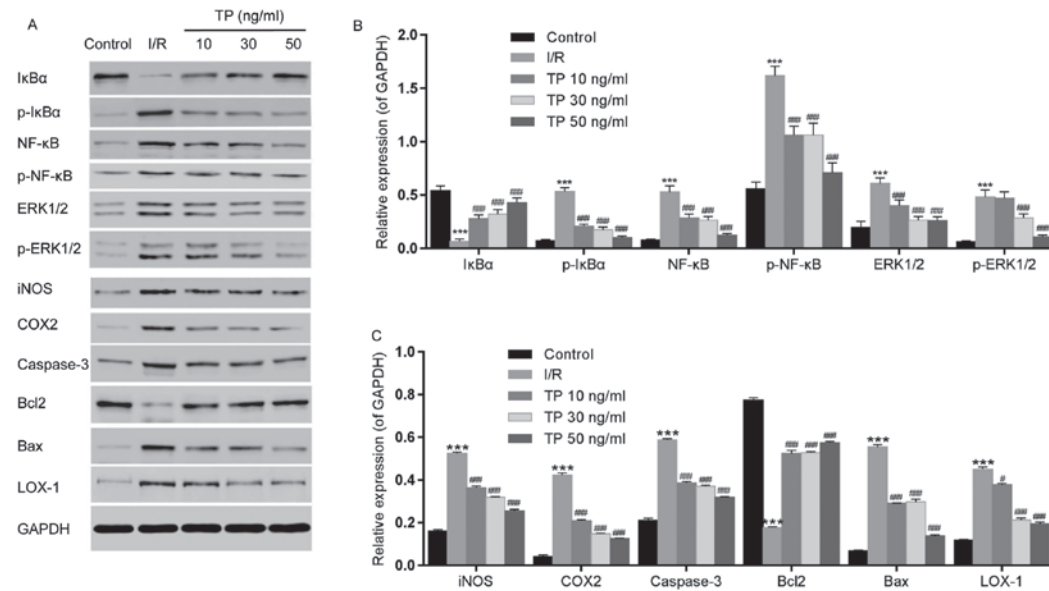


Figure 9. Effects of TP on the phosphorylation of IκBα, NF-κB and ERK1/2, and the expression of iNOS, COX2, caspase-3, Bcl2, Bax and LOX-1, as determined by western blot analysis. (A) Relative expression levels of IκBα, NF-κB, ERK1/2, iNOS, COX2, caspase-3, Bcl2, Bax and LOX-1 were determined. (B) Semi-quantification of western blot analysis was used to measure the phosphorylation of IκBα, NF-κB and ERK1/2. (C) Expression levels of iNOS, COX2, caspase-3, Bcl2, Bax and LOX-1 were analyzed by semi-quantification of western blot analysis. ***P<0.001, compared with the control group. #P<0.05, ###P<0.001, compared with the I/R group (n=3). Bax, Bcl2-associated X protein; Bcl2, B-cell lymphoma 2; COX2, cyclooxygenase 2; ERK1/2, extracellular signal-regulated kinase 1/2; IκBα, NF-κB inhibitor α; iNOS, inducible nitric oxide synthase; I/R, ischemia/reperfusion; LOX-1, lectin-like oxidized low-density lipoprotein receptor-1; NF-κB; nuclear factor-κB; p-, phosphorylated; TP, triptolide.

groups iNOS was decreased in a dose-dependent manner, thus indicating the inhibitory effects of TP during I/R.

COX2 and LOX-1 were measured using western blot analysis, in order to evaluate the peroxidative damage caused by I/R (Fig. 9A and C). COX2 and LOX-1 expression levels were increased following I/R, whereas in the TP-treated

groups COX2 and LOX-1 were decreased in a dose-dependent manner.

ERK1/2 phosphorylation was also detected by western blot analysis (Fig. 9A and B). The phosphorylation of ERK1/2 was increased in the I/R group, but decreased in the TP-treated groups. Furthermore, the expression levels of caspase-3 and

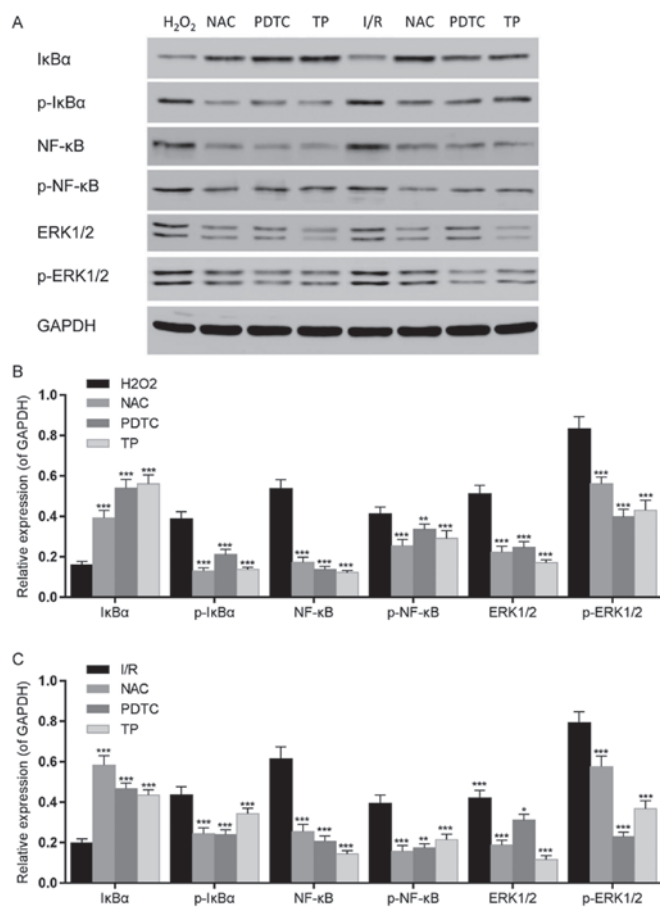


Figure 10. Effects of TP on I κ B α , NF- κ B and ERK1/2 phosphorylation in H9C2 cells, as evaluated by western blot analysis. (A) I κ B α , NF- κ B and ERK1/2 phosphorylation was detected by western blotting. (B) I κ B α , NF- κ B and ERK1/2 phosphorylation was semi-quantified after western blot analysis following treatment with H₂O₂ for 24 h. ***P*<0.01, ****P*<0.001, compared with the H₂O₂ group. (C) I κ B α , NF- κ B and ERK1/2 phosphorylation was semi-quantified after western blot analysis following 2 h of ischemia and 6 h of reperfusion. **P*<0.05, ***P*<0.01, ****P*<0.001, compared with the I/R group (n=3). ERK1/2, extracellular signal-regulated kinase 1/2; H₂O₂, hydrogen peroxide; I κ B α , NF- κ B inhibitor α ; I/R, ischemia/reperfusion; NAC, *N*-acetylcysteine; NF- κ B; nuclear factor- κ B; p-, phosphorylated; PDTTC, pyrrolidine dithiocarbamate; TP, triptolide.

Bax were increased in the I/R group compared with in the control group, whereas Bcl2 was decreased (Fig. 9A and C). Conversely, caspase-3 and Bax expression were decreased by TP in a dose-dependent manner, whereas Bcl2 was increased in the TP-treated groups, thus indicating the inhibitory effects of TP against cell apoptosis.

Discussion

In the present study, the protective effects of TP were determined against a rat model of I/R and H9C2 cardiac cells undergoing I/R. The results of the present study revealed the mechanisms underlying myocardial I/R injury. Conversely, TP-treated cardiac cells exhibited reduced cell swelling, necrosis and degeneration following I/R, and the production of proinflammatory cytokines, including TNF- α , IL-1 β and IL-6, was reduced, as was NF- κ B expression. In addition, attenuation of ROS generation induced by TP reduced the lipid peroxidation damage caused by I/R, thus suggesting the antioxidative effects of TP. Furthermore, ERK1/2 and caspase-3

were inhibited by TP, thus suggesting that TP suppressed the ERK1/2 pathway and inhibited cell apoptosis.

NF- κ B, which is regulated by I κ B α , is a transcription factor that controls the production and expression of numerous cytokines and chemokines (17). In addition, NF- κ B mediates cell apoptosis and inflammation in response to immunological stimuli. NF- κ B was previously reported to be significantly activated in cerebral I/R (18,19). Activated NF- κ B may upregulate the expression of proinflammatory cytokines, including TNF- α , IL-1 β and IL-6, thus resulting in inflammation. In the present study, phosphorylation of NF- κ B and I κ B α , and the expression of TNF- α , IL-1 β and IL-6, was measured in response to cardiac I/R. p-I κ B α accompanied by activated NF- κ B induced inflammation in H9C2 cells, which was relieved following TP treatment. NF- κ B deactivation was detected in the TP-treated groups, thus suggesting that TP inhibited activation of NF- κ B, which was followed by suppression of proinflammatory cytokines, TNF- α , IL-1 β and IL-6. Furthermore, similar results were obtained following administration of PDTTC, which was confirmed to act as an NF- κ B inhibitor. These data suggested that TP exerted similar effects as NF- κ B inhibitor. iNOS expression is involved in early inflammation, and is considered a response to tissue damage (20,21). In the present study, the expression levels of iNOS were increased during I/R and were attenuated in TP-pretreated H9C2 cells, thus suggesting the anti-inflammatory effects of TP. Furthermore, the percentage of TUNEL-positive cells was significantly reduced following treatment with TP. Therefore, these findings demonstrated the detrimental role of NF- κ B in myocardial ischemia, and the inhibitory effects of TP on NF- κ B.

MDA is a sensitive indicator of ROS-mediated lipid peroxidation, which contributes to I/R injury, whereas SOD and CAT are endogenous antioxidant enzymes that are developed to inhibit the production of ROS (22,23). It has previously been suggested that the development of ROS serves an important role in tissue damage caused by I/R. ROS in tissues that experience I/R are metabolized to prostaglandins and leukotrienes, which result in the chemotaxis of leukocytes, and control of vascular endothelial cell function, thus indicating the possible role of ROS-mediated lipid peroxidation in I/R injury. LOX-1 is an indicator of oxidative stress, which has been reported to present increased expression during tissue damage, whereas COX2 is the essential enzyme in prostaglandin synthesis (24-27). In the present study, elevated ROS levels were detected in tissue samples and H9C2 cells. The results obtained from biochemical analyses in rat tissues and H9C2 cells demonstrated that MDA levels were significantly increased, whereas SOD and CAT activity was decreased in response to I/R. These effects were markedly attenuated following treatment with TP in a dose-dependent manner, thus indicating that I/R induces injury via ROS-mediated lipid peroxidation. Furthermore, the expression levels of LOX-1 and COX2 were assessed by western blot analysis; LOX-1 and COX2 were increased during I/R, whereas their expression was attenuated by TP, thus indicating that I/R induced damage via lipid peroxidation and TP exerted protective effects against I/R. In addition, in order to explore the mechanism underlying ROS-induced damage and the mechanism underlying the protective effects of TP against I/R injury, H9C2 cells were treated with NAC, and ROS generation, MDA levels, and the activity levels of SOD and CAT, were assessed in response to H₂O₂-induced peroxidation damage. NAC, as a

ROS inhibitor, exerted inhibitory effects on ROS-mediated lipid peroxidation caused by H₂O₂. ROS generation was increased in H9C2 cells following treatment with H₂O₂; however, ROS levels were attenuated in NAC- and TP-treated groups. These findings support the hypothesis that ROS-mediated lipid peroxidation causes cardiac cell injury during I/R. The present study indicated that tissues may be damaged by I/R through ROS-mediated lipid peroxidation, whereas TP pretreatment could alleviate I/R injury by enhancing the activities of endogenous antioxidant enzymes, including CAT and SOD, in order to inhibit lipid peroxidation.

TUNEL and Annexin V/PI staining revealed that cell apoptosis was increased in response to I/R injury. Conversely, apoptotic rate was significantly decreased following TP pretreatment. In order to explore the mechanisms underlying I/R-induced cell apoptosis, numerous apoptosis-associated proteins, including Bcl2, Bax and caspase-3, were detected by western blot analysis. Caspase-3 is activated by apoptotic signals acts on peptide chain and split substrate, resulting in cell apoptosis. Caspase-3 serves a direct role in cell apoptosis as an effector caspase. It has been reported that caspase-3 induces activation of caspase-activated deoxyribonuclease (CAD), which is associated with DNA degradation (28). When apoptosis occurs, CAD is released by the inhibitor of CAD, which is activated by caspase-3. In addition, nuclear lamina, which is responsible for the stability of chromatin, may be cut by caspase-3 at a single site, thus resulting in chromatin degradation (29,30). Bax and Bcl2 belong to the Bcl2 family, which possess numerous highly conserved fragments that are mainly distributed in the nuclear membrane, endoplasmic reticulum and mitochondrial membrane (31). Bcl2 exerts an anti-apoptotic function by inhibiting the release of apoptosis-promoting substances from the mitochondria and suppressing activation of proapoptotic proteins, caspase-3 and Bax (32,33). Therefore, TP-induced Bcl2 upregulation, and caspase-3 and Bax downregulation, suggested that TP may suppress cell apoptosis. In addition, p-ERK1/2 was also assessed in the present study. It has been reported that reduced activation of the phosphoinositide 3-kinase-protein kinase B pathway in myocardial I/R may be accompanied by decreased ERK1/2 expression (34). The results of the present study corresponded with those in previous studies. ERK1/2 was downregulated in the I/R group, thus suggesting that the ERK1/2 pathway is inhibited during I/R; however, ERK1/2 expression was improved in TP-pretreated H9C2 cells, thus suggesting that ERK1/2 may be activated by TP so as to inhibit cell apoptosis during I/R injury.

Three different dosages of TP were used in the present study to investigate the association between the protective effects and dosage of TP, in order to provide a theoretical basis for clinical study. Data obtained from high-dose TP presented a significant difference compared with in the control group. The difference between the TP-treated groups and the control group may be due to the rapid absorption time and short half-life of TP. Reduced bioactivity of TP may affect the protective effects against I/R injury, which should be taken into account in future studies. Regardless, TP exerted efficient protective effects against I/R damage in cardiac cells.

In conclusion, the present study demonstrated that TP exerted protective effects on cardiac cells during I/R *in vivo* and *in vitro*. In addition, the mechanisms underlying the protective effects of TP, including anti-inflammatory action, antioxidation and apoptotic resistance, were investigated.

Acknowledgements

Not applicable.

Funding

The present study was funded by a grant from the National Natural Science Foundation of China (grant no. 81500285), Natural Science Foundation of Shanxi Province (grant no. 2011011041-1) and the Doctor Start-up Fund of Shanxi Medical University (grant no. 03201409).

Availability of data and materials

The analyzed data sets generated during the study are available from the corresponding author on reasonable request.

Authors' contributions

BY and BL conceived and designed the study. BY, PY, GZY, HLC and FW performed the experiments. BY and BL wrote the manuscript. All authors read and approved the manuscript.

Ethics approval and consent to participate

The present study was approved by the Institutional Animal Care and Use Committee (IACUC-20130315-01).

Consent for publication

Not applicable.

Competing interests

The authors declare that they have no competing interests.

References

- Durukan A and Tatlisumak T: Acute ischemic stroke: Overview of major experimental rodent models, pathophysiology, and therapy of focal cerebral ischemia. *Pharmacol Biochem Behav* 87: 179-197, 2007.
- Donnan GA, Fisher M, Macleod M and Davis SM: Stroke. *Lancet* 71: 1612-1623, 2008.
- Molina CA and Alvarez-Sabín J: Recanalization and reperfusion therapies for acute ischemic stroke. *Cerebrovasc Dis* 27 (Suppl 1): 162-167, 2009.
- Peralta C, Bulbena O, Xaus C, Prats N, Cutrin JC, Poli G, Gelpi E and Roselló-Catafau J: Ischemic preconditioning: A defense mechanism against the reactive oxygen species generated after hepatic ischemia reperfusion. *Transplantation* 73: 1203-1211, 2002.
- Eltzschig HK and Eckle T: Ischemia and reperfusion-from mechanism to translation. *Nat Med* 17: 1391-1401, 2011.
- Huang J, Upadhyay UM and Tamargo RJ: Inflammation in stroke and focal cerebral ischemia. *Surg Neurol* 66: 232-245, 2006.
- Esterbauer H and Cheeseman KH: Determination of aldehydic lipid peroxidation products: Malonaldehyde and 4-hydroxynonenal. *Methods Enzymol* 186: 407-421, 1990.
- Tuttolomondo A, Di Sciacca R, Di Raimondo D, Renda C, Pinto A and Licata G: Inflammation as a therapeutic target in acute ischemic stroke treatment. *Curr Top Med Chem* 9: 1240-1260, 2009.
- Faul JL, Nishimura T, Berry GJ, Benson GV, Pearl RG and Kao PN: Triptolide attenuates pulmonary arterial hypertension and neointimal formation in rats. *Am J Respir Crit Care Med* 162: 2252-2258, 2000.

10. Hao M, Li X, Feng J and Pan N: Triptolide protects against ischemic stroke in rats. *Inflammation* 38: 1617-1623, 2015.
11. Hoyle GW, Hoyle CI, Chen J, Chang W, Williams RW and Rando RJ: Identification of triptolide, a natural diterpenoid compound, as an inhibitor of lung inflammation. *Am J Physiol Lung Cell Mol Physiol* 298: L830-L836, 2010.
12. Wu C, Xia Y, Wang P, Lu L and Zhang F: Triptolide protects mice from ischemia/reperfusion injury by inhibition of IL-17 production. *Int Immunopharmacol* 11: 1564-1572, 2011.
13. He JK, Yu SD, Zhu HJ, Wu JC and Qin ZH: Triptolide inhibits NF-kappaB activation and reduces injury of donor lung induced by ischemia/reperfusion. *Acta Pharmacol Sin* 28: 1919-1923, 2007.
14. Lin N, Liu C, Xiao C, Jia H, Imada K, Wu H and Ito A: Triptolide, a diterpenoid triepoxide, suppresses inflammation and cartilage destruction in collagen-induced arthritis mice. *Biochem Pharmacol* 73: 136-146, 2007.
15. Lu Y, Liu Y, Fukuda K, Nakamura Y, Kumagai N and Nishida T: Inhibition by triptolide of chemokine, proinflammatory cytokine, and adhesion molecule expression induced by lipopolysaccharide in corneal fibroblasts. *Invest Ophthalmol Vis Sci* 47: 3796-3800, 2006.
16. Matta R, Wang X, Ge H, Ray W, Nelin LD and Liu Y: Triptolide induces anti-inflammatory cellular responses. *Am J Transl Res* 1: 267-282, 2009.
17. Chandel NS, Trzyna WC, McClintock DS and Schumacker PT: Role of oxidants in NF-kappa B activation and TNF-alpha gene transcription induced by hypoxia and endotoxin. *J Immunol* 165: 1013-1021, 2000.
18. Lakhan SE, Kirchgessner A and Hofer M: Inflammatory mechanisms in ischemic stroke: Therapeutic approaches. *J Transl Med* 7: 97, 2009.
19. Jin XQ, Ye F, Zhang JJ, Zhao Y and Zhou XL: Triptolide attenuates cerebral ischemia and reperfusion injury in rats through the inhibition the nuclear factor kappa B signaling pathway. *Neuropsychiatr Dis Treat* 11: 1395-1403, 2015.
20. Hur GM, Ryu YS, Yun HY, Jeon BH, Kim YM, Seok JH and Lee JH: Hepatic ischemia/reperfusion in rats induces iNOS gene transcription by activation of NF-kappaB. *Biochem Biophys Res Commun* 261: 917-922, 1999.
21. Kim ID, Sawicki E, Lee HK, Lee EH, Park HJ, Han PL, Kim KK, Choi H and Lee JK: Robust neuroprotective effects of intranasally delivered iNOS siRNA encapsulated in gelatin nanoparticles in the postischemic brain. *Nanomedicine* 12: 1219-1229, 2016.
22. Murakami K, Kondo T, Kawase M, Li Y, Sato S, Chen SF and Chan PH: Mitochondrial susceptibility to oxidative stress exacerbates cerebral infarction that follows permanent focal cerebral ischemia in mutant mice with manganese superoxide dismutase deficiency. *J Neurosci* 18: 205-213, 1998.
23. Wu C, Wang P, Rao J, Wang Z, Zhang C, Lu L and Zhang F: Triptolide alleviates hepatic ischemia/reperfusion injury by attenuating oxidative stress and inhibiting NF-kB activity in mice. *J Surg Res* 166: e205-e213, 2011.
24. Shiraki T, Aoyama T, Yokoyama C, Hayakawa Y, Tanaka T, Nishigaki K, Sawamura T and Minatoguchi S: LOX-1 plays an important role in ischemia-induced angiogenesis of limbs. *PLoS One* 9: e114542, 2014.
25. Mao X, Xie L and Greenberg DA: Effects of flow on LOX-1 and oxidized low-density lipoprotein interactions in brain endothelial cell cultures. *Free Radic Biol Med* 89: 638-641, 2015.
26. Ozturk H, Gezici A and Ozturk H: The effect of celecoxib, a selective COX-2 inhibitor, on liver ischemia/reperfusion-induced oxidative stress in rats. *Hepatol Res* 34: 76-83, 2006.
27. Du Y, Zhu Y, Teng X, Zhang K, Teng X and Li S: Toxicological effect of manganese on NF-kB/iNOS-COX-2 signaling pathway in chicken testes. *Biol Trace Elem Res* 168: 227-234, 2015.
28. Weng C, Li Y, Xu D, Shi Y and Tang H: Specific cleavage of Mcl-1 by caspase-3 in tumor necrosis factor-related apoptosis-inducing ligand (TRAIL)-induced apoptosis in Jurkat leukemia T cells. *J Biol Chem* 280: 10491-10500, 2005.
29. Lavrik IN, Golks A and Krammer PH: Caspases: Pharmacological manipulation of cell death. *J Clin Invest* 115: 2665-2672, 2005.
30. Stennicke HR and Salvesen GS: Biochemical characteristics of caspases-3, -6, -7, and -8. *J Biol Chem* 272: 25719-25723, 1997.
31. Hsu YT, Wolter KG and Youle RJ: Cytosol-to-membrane redistribution of Bax and Bcl-X(L) during apoptosis. *Proc Natl Acad Sci USA* 94: 3668-3672, 1997.
32. Nechushtan A, Smith CL, Hsu YT and Youle RJ: Conformation of the Bax C-terminus regulates subcellular location and cell death. *EMBO J* 18: 2330-2341, 1999.
33. Shi Y, Chen J, Weng C, Chen R, Zheng Y, Chen Q and Tang H: Identification of the protein-protein contact site and interaction mode of human VDAC1 with Bcl-2 family proteins. *Biochem Biophys Res Commun* 305: 989-996, 2003.
34. Duan M, Wang ZC, Wang XY, Shi JY, Yang LX, Ding ZB, Gao Q, Zhou J and Fan J: TREM-1, an inflammatory modulator, is expressed in hepatocellular carcinoma cells and significantly promotes tumor progression. *Ann Surg Oncol* 22: 3121-3129, 2015.



This work is licensed under a Creative Commons Attribution-NonCommercial-NoDerivatives 4.0 International (CC BY-NC-ND 4.0) License.